Applications and Applied Mathematics: An International Journal (AAM)

Volume 14
Issue 4 *Special Issue No. 4 (March 2019)*

Article 1

3-2019

MHD Boundary Layer Flow and Heat Transfer to Sisko Nanofluid Past a Nonlinearly Stretching Sheet with Radiation

Macha Madhu
Kuvempu University

B. J. Gireesha
Kuvempu University

Naikoti Kishan
Osmania University

Available at
http://pvamu.edu/aam
Appl. Appl. Math.
ISSN: 1932-9466

Applications and Applied Mathematics:
An International Journal
(AAM)

Special Issue No. 4 (March 2019), pp. 1 – 15

MHD Boundary Layer Flow and Heat Transfer to Sisko Nanofluid Past a Nonlinearly Stretching Sheet with Radiation

[1]**Macha Madhu**, [2]**B.J. Gireesha, and** [3]**Naikoti Kishan**

[1,2] Department of Studies and Research in Mathematics
Kuvempu University
Jnansahyadri-577451
Shimoga, Karnataka
[1]madhumaccha@gmail.com

[3]Department of Mathematics
Osmania University
Hyderabad-07
Telangana, India

Received: August 8, 2018; Accepted: October 28, 2018

Abstract

The steady flow of a Sisko fluid model in the presence of nanoparticles is studied. The governing partial differential equations are converted to a set of coupled non-linear ordinary differential equations by using suitable similarity transformations. Numerical solutions for the coupled non-linear ordinary differential equations are carried out by a variational finite element method. A suitable comparison has been made with previously published results in the literature as a limiting case of the considered problem. The comparison confirmed an excellent agreement. The results for the local Nusselt number are tabulated and discussed. Behavior of essential physical parameters are presented graphically and discussed for velocity, temperature and nanoparticle volume fraction.

Keywords: Non-Newtonian; nanofluid; Brownian motion; Sisko fluid; thermophoresis; FEM

MSC 2010 No.: 76A05, 74S05, 80A20

1. Introduction

Over the past two decades, much attention has been paid to the study of non-Newtonian fluids because of their profuse industrial and technological applications. There is a vast utility of non-

Newtonian fluids in industrial sector such as pharmaceutical, polymer, personal care products and so forth. It is a broad class of fluids so there is not a single model that can describe all the properties of non-Newtonian fluids. Therefore several constitutive equations are proposed to predict the physical structure and behavior of such fluids. Among these, a comparatively simple model, named Sisko fluids, is capable of describing shear thinning and thickening phenomena, which commonly exists in nature. Such fluids are well known and have many industrial applications. It is the most appropriate model for the flow of greases. Waterborne coatings and metallic automotive base coat, where polymeric suspensions are used cement slurries, lubricating greases, most pseudo-plastic fluids and drilling fluids are some of its industrial applications (Sisko (1958), Siddiqui et al. (2009), Mekheimer and El Kot (2012)). Sajid and Hayat (2008) examined wire coating analysis by withdrawal from a bath of Sisko fluid which was established that Sisko fluid is a non-Newtonian fluid which has no closed form solution and also affected by flow parameters in the flow regime. Recently, Talay et al. (2009) examined the implicit differential equation arising in the steady flow of a Sisko fluid which re-established the nonlinearity of the fluid.

However a good number of fluid rheology are already in existence, particularly for most of those fluids used as lubricants and having non-Newtonian behavior, the flow can be analyzed with the help of a power-law model. Furthermore, a power-law fluid model characterizes both pseudo-plastic and dilatant fluids-two important classes of non-Newtonian lubricants and again can characterize Newtonian fluid as a special case. It is because of such wide coverage in the analysis of lubricants together with its mathematical simplicity that the Sisko fluid model (Sisko (1958)) has been preferred for application in the present problem.

The interest in heat transfer problems involving power-law non-Newtonian fluids has grown in the past half century since heat transfer process plays an important role in industrial and technological applications. This is due to the fact that the rate of cooling influences a lot to the quality of the final product with desired characteristics such as metal extrusion, glass fiber production hot rolling, manufacturing of plastic and rubber sheets and so forth.

Consequently, the results for the flows and heat transfer of non-Newtonian fluids are needed. Some recent studies dealing with heat transfer of non-Newtonian fluids may be mentioned in the references Zhang et al. (2008) and Hayat et al. (2008). Kishan and Shashidhar Reddy (2013) investigated MHD effects on non-Newtonian power-law fluid past a continuously moving porous flat plate. Kavitha and Kishan (2014) studied MHD flow and heat transfer of non-Newtonian power-law fluid over a stretching surface with viscous dissipation.

The constitutive equations of non-Newtonian fluids involve rheological parameters. Except in the case of some basic flows, the constitutive equations of non-Newtonian fluids give rise to more complexities in the momentum equation. The resulting equations are of higher order than the Navier-Stokes equations and the adherence boundary conditions are insufficient for the determinacy (Rajagopal (1995)). The equations of non-Newtonian fluids are much complicated and making the task of obtaining the accurate solutions is a difficult one. Moreover the magnetohydrodynamic (MHD) features of non-Newtonian fluids add further complications in the governing equations. Such flow of an electrically conducting fluid under the action of a constant magnetic field has applications in many devices such as MHD power generators, MHD pumps and accelerators, etc. Examples include flow of nuclear fuel slurries, flow of liquid metals and alloys, flow of plasma, flow of mercury amalgams, lubrications of heavy oils and greases.

Many engineering and industrial processes involve heat transfer by means of a flowing fluid in either laminar or turbulent regimes. A decrease in thermal resistance of heat transfer in the fluids would significantly benefit many of these applications/processes. Nanofluids have the potential to reduce thermal resistances, and industrial groups such as electronics, medical, food and manufacturing would benefit from such improved heat transfer.

It is well known that conventional heat transfer fluids, such as oil, water and ethylene glycol mixture, are poor heat transfer fluids. Choi (1995) introduced the technique of nanofluids by using a mixture of nanoparticles and the base fluids. The presence of the nanoparticles in the nanofluid increases the thermal conductivity and therefore substantially enhances the heat transfer characteristics of the nanofluid. Nanotechnology has been an ongoing hot topic of discussion in public health as researchers claim that nanoparticles could present possible dangers in health and environment, Mnyusiwalla et al. (2003). There are several numerical studies on the modelling of natural convection heat transfer in nanofluids (Kakac and Pramuanjaroenkij (2009), Godson et al. (2010), Olanrewaju et al. (2012)), Gbadeyan et al. (2011) numerically studied boundary layer flow induced in a nanofluid due to a linearly stretching sheet in the presence of thermal radiation and induced magnetic field. There are numerous biomedical applications that involve nanofluids such as magnetic cell separation, drug delivery, hyperthermia, and contrast enhancement in magnetic resonance imaging.

In most of the previous investigations, Newtonian fluids were used as base fluids. Non-Newtonian nanofluids (non-Newtonian fluids with dispersed nanoparticles) have been used by only few researchers including Chen et al. (2007), Ding et al. (2007), and Chen et al. (2008). More work is needed to investigate the characteristics of nanofluids and the mechanism of the forced convective heat transfer of nanofluids. Hamad and Bashir (2009) studied the forced convection heat transfer to the power-law non-Newtonian nanofluid from the stretching surface.

Only a few have started considering the non-Newtonian characteristics of nanofluid (see Hojjat et al. (2008, 2011)). Madhu and Kishan (2016) investigated MHD mixed convection stagnation-point flow of a non-Newtonian power-law nanofluid towards a stretching surface. Nield (2011) studied the onset of convection in a layer of a porous medium which is filled with non-Newtonian nanofluids of power-law type. Ellahi et al. (2012) have elaborated that non-Newtonian nanofluids have potential roles in physiological transport as biological solutions and also in polymer melts, paints, etc. Recently, Masood Khan et al. (2015) investigated Sisko nanofluid over non-linearly stretching sheet.

The principal aim of this paper is to study the boundary layer magnetic boundary layer flow of a Sisko nanofluid over a non-linear stretching sheet with radiation. We considered revised boundary conditions of nanofluid model introduced by Kuzenostava and Nield (2014). The uniform magnetic field applied along a sheet and the influence of thermal radiation is considered. The governing equations are solved numerically by using variational finite element method.

2. Mathematical Formulation

Consider the steady two-dimensional flow of an electrically conducting incompressible Sisko nanofluid over a stretching sheet coinciding with the plane $y = 0$. The flow is confined to the region $y > 0$ and is generated due to the stretching of the sheet and the sheet stretching with the non-linear velocity $U = cx^m$, where c is the constant and m is the stretching rate of the sheet. Stretching velocity is produced by applying two equal and opposite forces on the sheet such that origin is kept constant. The steady laminar two-dimensional flow of Sisko nanofluid is governed by the following equations:

$$\frac{\partial u}{\partial x} + \frac{\partial v}{\partial y} = 0, \tag{1}$$

$$u\frac{\partial u}{\partial x} + v\frac{\partial u}{\partial y} = \frac{a}{\rho}\frac{\partial^2 u}{\partial y^2} - \frac{b}{\rho}\frac{\partial}{\partial y}\left(-\frac{\partial u}{\partial y}\right)^n - \frac{\sigma B_0^2}{\rho}u, \tag{2}$$

$$u\frac{\partial T}{\partial x} + v\frac{\partial T}{\partial y} = \alpha\frac{\partial^2 T}{\partial y^2} + \tau\left[D_B\frac{\partial C}{\partial y}\frac{\partial T}{\partial y} + \frac{D_T}{T_\infty}\left(\frac{\partial T}{\partial y}\right)^2\right] - \frac{1}{\rho C_p}\frac{\partial q_r}{\partial y}, \tag{3}$$

$$u\frac{\partial C}{\partial x} + v\frac{\partial C}{\partial y} = D_B\frac{\partial^2 C}{\partial y^2} + \frac{D_T}{T_\infty}\frac{\partial^2 T}{\partial y^2}. \tag{4}$$

The relevant boundary conditions of the problem are:

$$u = U = cx^m, \quad v = 0, \quad T = T_w, \quad D_B\frac{\partial C}{\partial y} + D_T\frac{\partial T}{\partial y} = 0 \quad \text{at} \quad y = 0, \tag{5a}$$

$$u \to 0, \quad T \to T_\infty, \quad C \to C_\infty \quad \text{at} \quad y \to \infty, \tag{5b}$$

where, u and v are the velocity components of fluid along the x and y directions, respectively. Here a, b and $n(> 0)$ are the material constants of the Sisko fluid. T is the temperature of the fluid, C is the nanoparticle volume fraction σ is the electric conductivity, ρ is the fluid density, α_m is the thermal diffusivity, D_B is the Brownian diffusion coefficient, D_T is the thermophoretic diffusion coefficient and B_0 is the magnetic field. Using the Rosseland approximation for radiation, the radiative heat flux is simplified as:

$$q_r = -\frac{4\sigma_1}{3\chi}\frac{\partial T^4}{\partial y}, \tag{6}$$

where σ_1 and χ are the Stefan-Boltzmann constant and the mean absorption coefficient, respectively. It has been assumed that the temperature differences within the flow, such as the term T^4, may be expressed as a linear function of temperature. Hence, expanding T^4 in a Taylor series about a free stream temperature T_∞ and neglecting higher-order terms, we get:

$$T^4 = 4T_\infty^4 T - 3T_\infty^4. \tag{7}$$

Using (6) and (7) in the last term of equation (3), it gives

$$\frac{\partial q_r}{\partial y} = -\frac{16\sigma_1 T_\infty^3}{3\chi}\frac{\partial^2 T}{\partial y^2}. \tag{8}$$

We introduce the following local similarity variable transformation,

$$\psi = Ux\left(Re_b\right)^{-\frac{1}{n+1}} f(\eta), \theta = \frac{T-T_\infty}{T_w-T_\infty}, \phi = \frac{C-C_\infty}{C_\infty}, \eta = \frac{y}{x}\left(Re_b\right)^{\frac{1}{n+1}}. \tag{9}$$

where η is similarity variable and ψ is stream function defined by $u = \frac{\partial\psi}{\partial y}$ and $v = -\frac{\partial\psi}{\partial x}$. The local Reynolds numbers is defined by $Re_a = \frac{\rho x U}{a}$ and $Re_b = \frac{\rho U^{2-n} x^n}{b}$. Using local similarity transformations (9), equations $(2)-(4)$ transformed to

$$Sf''' + n\left(-f''\right)^{(n-1)} f''' + \left(\frac{2mn-m+1}{n+1}\right) ff'' - mf'^2 - Mf' = 0, \tag{10}$$

$$\frac{1}{Pr}\left(1+\frac{4R_d}{3}\right)\theta'' + \left(\frac{2mn-m+1}{n+1}\right) f\theta' + Nb\theta'\phi' + Nt\theta'^2 = 0, \tag{11}$$

$$\phi'' + \left(\frac{2mn-m+1}{n+1}\right) Lef\phi' + \frac{Nt}{Nb}\theta'' = 0. \tag{12}$$

The boundary conditions are transformed as:

$$f' = 1, \;\; f = 0, \;\; \theta = 1, \;\; Nb\phi' + Nt\theta' = 0 \quad \text{at} \quad \eta = 0, \tag{13a}$$

$$f' \to 0, \;\; \theta \to 0, \;\; \phi \to 0 \quad \text{at} \quad \eta \to \infty. \tag{13b}$$

In the above equations $S = \frac{Re_b^{2-n}}{Re_a}$ is the material parameter of the Sisko fluid, $M = \frac{\sigma B_0^2}{\rho b}$ magnetic parameter, $Pr = \frac{Ux}{\alpha}\left(Re_b\right)^{\frac{-2}{n+1}}$ is the Prandtl number, $R_d = \frac{4\sigma_1 T_\infty^3}{k\chi}$ is radiation parameter, $Nb = \frac{\tau D_B C_\infty}{Ux}\left(Re_b\right)^{\frac{2}{n+1}}$ is the Brownian motion $Nt = \frac{\tau D_T (T_w - T_\infty)}{UxT_\infty}\left(Re_b\right)^{\frac{2}{n+1}}$ is the thermophoresis parameter and $Le = \frac{Ux}{D_B}\left(Re_b\right)^{\frac{-2}{n+1}}$ is the Lewis number. The physical quantity of major interest is the local skin friction coefficient and local Nusselt number in non-dimensional form is given by

$$\frac{1}{2}\left(Re_b\right)^{\frac{2}{n+1}} C_{f_x} = Sf''(0) - \left(-f''(0)\right)^n, \quad \left(Re_b\right)^{\frac{-2}{n+1}} Nu_x = -\theta'(0). \tag{14}$$

3. Method of solution

The finite element method is a powerful technique for solving ordinary or partial differential equations. The steps involved in the finite element analysis are as follows:

- Discretization of the domain into elements,
- Derivation of element equations,
- Assembly of Element Equations,
- Imposition of boundary conditions,
- Solution of assembled equations.

The entire flow domain is divided into 1000 linear elements of equal size, each element has two nodes. At each node four functions are to be evaluated, hence after assembly of all the elemental equations, we obtain a matrix of the order 4004×4004. The obtained system is non-linear, therefore an iterative scheme is utilized in the solution. After imposing the boundary conditions the remaining system contains 3997 equations, which is solved by the Gauss elimination method while maintaining an accuracy of 10^{-5}.

4. Results and discussion

The extensive computations have been performed to analyze the influence of the physical parameters namely power-law index n, magnetic field parameter M, Sisko parameter S, non-linear stretching parameter m, thermophoresis parameter Nt, Brownian motion Nb, radiation parameter Rd and Lewis number Le are presented through Figures 1-8 for dimensionless velocity, temperature and nanoparticle volume fraction parameter. Moreover the dimension less heat and mass transfer coefficients are reported in Table 2. Table 1 reports the comparison between present results and previously published results of Khan and Pop (2010), Wang (1989), and Masood Khan et al. (2015). There is a good agreement of present results and authenticate the validity of the present results. The variations in the numerical values of local Nusselt number are provided in Table 2 for various flow controlling parameters. It is evident that local Nusselt number $-\theta'(0)$ increases by increasing n, M, Rd, Nt and Le but decreases for increasing in S value.

The impact of non-linear stretching parameter m on velocity, temperature and nanoparticle volume fraction profiles respectively, is depicted through Figures 1(a)-(c) for pseudo-plastic, Newtonian and dilatant fluids. It is anticipated by these figures that velocity and temperature distribution diminishes as increasing stretching sheet parameter m for both Newtonian and non-Newtonian fluids. From Figure 1(c) it should be noticed that the nanoparticle volume fraction profiles decreases with the increase of m far away from the boundary while nanoparticle volume fraction profiles increases with the increase of m in the vicinity of the boundary is noticed for both Newtonian and non-Newtonian fluids. It is interesting to note that the stretching sheet parameter m effect is higher in dilatant fluids when compared with pseudo-plastic fluids.

Figures 2(a)-(c) are depicted for the influence of magnetic field parameter M on velocity, temperature and nanoparticle volume fraction profiles respectively for pseudo-plastic, Newtonian and dilatant fluids. It appears from Figure 2(a) that an increase in the value of magnetic parameter M decreases the velocity profiles for both Newtonian and non-Newtonian fluids. This is because of the Lorentz force which resist force that acts in the direction opposite to the flow direction. This resist force slow down the fluid motion. Also, we can note that from Figure 2(b) the temperature distribution enhances with an increase in M. Further these figures portray that the boundary layer thickness becomes thin as magnetic parameter M increases, where as the thermal boundary layer thickness increases. The influence of magnetic parameter M is to enhances the nanoparticle volume fraction profiles is noticed from Figure 2(c).

The effects of Sisko fluid parameter S on the velocity, temperature and concentration profile for pseudo plastic, Newtonian and dilatant fluids are exhibited in Figures 3(a)-(c) respectively. In this study we have considered the values of Sisko fluid parameter S with the increase values of Sisko fluid parameter S, the fluid velocity increase for both Newtonian and non-Newtonian fluids, but the temperature profiles decreases in this case. The effect of Sisko fluid parameter S leads to decreases the concentration profiles. It is worth mentioning that Sisko parameter effect is more in pseudo plastic fluids for velocity, temperature as well as concentration profiles when compared with the Newtonian and dilatant fluids.

Figure 4(a) and 4(b) corresponds to the temperature and nanoparticle volume fraction profiles for different values of thermophoresis parameter Nt for pseudo-plastic, Newtonian and dilatant fluids. It is clear from these figures that the temperature profiles increases with an increase in Nt. However, we noticed that the influence of thermophoresis parameter Nt is enhance the nanoparticle volume fraction profiles significantly away from the boundary layer and the reverse phenomena is noticed near the sheet.

The impact of Brownian motion parameter Nb on the nanoparticle volume fraction profiles for pseudo-plastic, Newtonian and dilatant fluids is shown in Figure 5. In thermal conduction the motion of nanoparticles plays a pivotal role. Physically, the brownian motion is stronger incase of smaller nanoparticles which corresponds to larger the Nb value and reverse is the situation for smaller values of Nb. Due to chaotic motion of the nanoparticles (i.e. for larger Nb). For smaller values of Nb larger concentration boundary layer thickness is produced.

Figures 6(a)-(c) shows the velocity, temperature and nanoparticle volume fraction profiles for different power-law index n. These figures reveals that velocity profiles decreases for large values of the power-law index n for both cases (i.e. Newtonian and non-Newtonian fluids) also the temperature profiles decreases with the increase on n. The power-law index n is to decrease the nanoparticle volume fraction profiles far away from the sheet while it increases near the plate.

Figure 7 represents the temperature profiles for the different values of radiation parameter Rd. From these figures it can be noticed that with the increase in radiation parameter Rd is to increase the temperature profiles. The nanoparticles volume fraction profiles is decreased due to the increasing of Lewis number Le can be observed from Figure 8. Lewis number is inversely proportional to the Brownian diffusion coefficient. Brownian diffusion coefficient is weaker for higher Lewis number. This weaker Brownian diffusion coefficient creates a reduction in concentration profile.

5. Conclusion

In this work, we analyzed the problem of steady, boundary layer flow and heat transfer of Sisko nanofluid over a stretching surface under the influence of thermal radiation. From this investigation, the following conclusions can be drawn.

An increase in Sisko fluid parameter S enhances the velocity profiles but reduces temperature and nanoparticle volume fraction profiles. The velocity, temperature and nanoparticle volume fraction profile decreases with the rise in values of power-law index n and non-linear stretching parameter m. The influence of Brownian motion Nb, Lewis number Le is to decrease in nanoparticle volume fraction profiles for both Newtonian and non-Newtonian fluids. The radiation parameter Rd and thermophoresis parameter Nt have significant effect on dimensionless temperature and local Nusselt number.

Table 1. Comparison of local Nusselt number $-\theta'(0)$ for the case of Newtonian fluid with the results of Khan and Pop (2010), Wang (1989) and Masood Khan et al. (2015).

Pr	Present results	Khan and Pop (2010)	Wang (1989)	Masood Khan et al. (2015)
0.7	0.45411	0.4539	0.4539	0.45392
2.0	0.91129	0.9113	0.9124	0.91135
7.0	1.89621	1.8954	1.8954	1.89543
20.0	3.35405	3.3539	3.3539	3.35395

Table 2. Computations of the local Nusselt number for various values of n, S, M, Rd, Nb, Nt, and Le.

n	S	M	Rd	Nb	Nt	Le	$-\theta'(0)$
0.6	1.5	1.0	0.1	0.1	0.1	5	-0.788054
1.0							-0.776686
1.6							-0.768898
0.6	0.2						-0.773486
	0.4						-0.800226
	0.6						-0.819650
		1.5					-0.749480
		2.0					-0.716499
		2.5					-0.687815
			1.0				-0.500582
			2.0				-0.379913
			3.0				-0.321018
				0.3			-0.788054
				0.5			-0.788054
				0.7			-0.788054
					0.3		-0.716317
					0.5		-0.649114
					0.7		-0.587179
						2	-0.803261
						4	-0.792040
						6	-0.784760

REFERENCES

Akyildiz, F.T., Vajravelu, K., Mohapatra, R. N., Sweet, E. and Van Gorder, R. A. (2009). Implicit differential equation arising in the steady flow of a Sisko fluid, Applied Mathematics and Computation, Vol. 210, pp. 189-196.

Chen, H., Ding, Y. and Tan, C. (2007). Rheological Behaviour of Nanofluids, New J. Phys, Vol. 9, pp. 367.

Chen, H., Yang, W., He, Y., Ding, Y., Zhang, L., Tan, C., Lapkin, A.A. and Bavykin, D.V. (2008). Heat Transfer and Flow Behavior of Aqueous Suspensions of Titanate Nanotubes (Nanofluids), Powder Technol., Vol. 183, pp. 63-72.

Choi, S.U.S. (1995). Enhancing thermal conductivity of fluids with nanoparticles. In: Developments and Applications of Non-Newtonian Flows, FED, Vol. 231/MD, pp. 99-105.

Ding, Y., Chen, H., He, Y., Lapkin, A., Yeganeh, M., Siller, L. and Butenko, Y.V. (2007). Forced Convective Heat Transfer of Nanofluids, Adv. Powder Technol., Vol. 18, pp. 813-824.

Ellahi, R., Raza, M. and Vafai, K. (2012). Series solutions of non-Newtonian nanofluids with Reynold's model and Vogel's model by means of the homotopy analysis method, Mathematical and Computer Modelling, Vol. 55, pp. 1876-1891.

Gbadeyan, J.A, Olanrewaju, M.A. and Olanrewaju, P.O. (2011). Boundary layer flow of a nanofluid past a stretching sheet with a convective boundary condition in the presence of magnetic field and thermal radiation, Aust. J. Basic Appl. Sci., Vol. 5, pp. 1323-1334.

Godson, L., Raja, B., Lal, D.M. and Wongwises, S. (2010). Enhancement of heat transfer using nanofluid - An overview, Renew, Sustain. Energy Rev., Vol. 14, pp. 629-641.

Hamad, M.A.A. and Bashir M.A. (2009). Boundary-layer flow and heat transfer of a power-law non-Newtonian over a vertical stretching sheet, World Appl. Sci. J., Vol. 7, pp. 172-178.

Hayat, T., Noreen, S. and Sajid, M. (2008). Heat transfer analysis of the steady flow of a fourth grade fluid, Int. J. Theor. Sci., Vol. 47, pp. 591-599.

Hojjat, M., Etemad, S.G. and Bagheri, R. (2010). Laminar heat transfer of non-Newtonian nanofluids in a circular tube, Korean J. Chem. Eng., Vol. 27, pp. 1391-1396.

Hojjat, M., Etemad, S.G., Bagheri, R. and Thibault, J. (2011). Laminar convective heat transfer of non-Newtonian nanofluids with constant wall temperature, Heat Mass Transfer, Vol. 47, pp. 203-209.

Kakac, S. and Pramuanjaroenkij, A. (2009). Review of convective heat transfer enhancement with nanofluids, Int. J. Heat Mass Transf, Vol. 52, pp. 3187-3196.

Kavitha, P. and Kishan, N. (2014). MHD flow of a non-Newtonian power-law fluid over a stretching sheet with thermal radiation, viscous dissipation and slip boundary conditions, Acta Technica, Vol. 59, pp. 355-376.

Khan, M., Malik, R., Munir, A. and Khan, W.A. (2015). Flow and Heat Transfer to Sisko Nanofluid over a Nonlinear Stretching Sheet, Plos one, Vol. 10.

Khan, W.A. and Pop, I. (2010). Boundary-layer flow of a nanofluid past a stretching sheet, Int J Heat Mass Transf, Vol. 53, pp. 2477-2483.

Kishan, N. and Shashidhar, Reddy B. (2013). MHD effects on non-Newtonian power-law fluid past a continuously moving porous flat plate with heat flux and viscous dissipation, IJAME, Vol. 18, pp. 425-445.

Kuznetsov, A.V. and Nield, D.A. (2014). Natural convective boundary-layer flow of a nanofluid past a vertical plate: A revised model, International Journal of Thermal Sciences, Vol. 77, pp. 126-129.

Madhu, M. and Kishan, N. (2016). Finite Element Analysis of heat and mass transfer by MHD mixed convection stagnation-point flow of a non-Newtonian power-law nanofluid towards a stretching surface with radiation, Journal of the Egyptian Mathematical Society, Vol. 24, pp.

458-470.

Mekheimer, Kh.S. and El Kot, M.A. (2012). Mathematical modelling of unsteady flow of a Sisko fluid through an anisotropically tapered elastic arteries with time-variant overlapping stenosis, Appl. Math. Modell, Vol. 36, pp. 5393-5407.

Mnyusiwalla, A., Daar, A.S. and Singer, P.A. (2003). Mind the gap: science and ethics in nanotechnology, Nanotechnology, Vol. 14, pp. R9-R13.

Nield, D.A. (2011). A note on the onset of convection in a layer of a porous medium saturated by a non-Newtonian nanofluids of power-law type Transp, Porous Media, Vol. 87, pp. 121-123.

Olanrewaju, P.O., Olanrewaju, M.A. and Adesanya, A.O. (2012). Boundary layer flow of nanofluids over a moving surface in a flowing fluid in the presence of radiation, Int. J. Appl. Sci. Technol., Vol. 2, pp. 274-285.

Rajagopal, K.R. (1995). Navier-Stokes equations and related nonlinear problems (Ed. A. Sequeira), Plenum Press, New York, pp. 273.

Sajid, M., Hayat, T. (2008). Wire coating analysis by withdrawal from a bath of Sisko Fluid, Applied Mathematics and Computation, Vol. 199, pp. 13-22.

Siddiqui, A.M., Ansari, A.R., Ahmad, A. and Ahmad, N. (2009). On Taylor's scraping problem and flow of Sisko fluid, Mathematical Modeling and Analysis, Vol. 14, pp. 515-529.

Sisko, A.W. (1958). The flow of lubricating greases, Industrial and Engineering Chemistry Research, Vol. 50, pp. 1789-1792.

Wang, C.Y. (1989). Free convection on a vertical stretching surface, J Appl Math Mech (ZAMM), Vol. 69, pp. 418-420.

Zhang, M., Shen, X., Ma, J. and Zhang, B. (2008). Theoretical analysis of convective heat transfer of Oldroyd-B fluid in a curved pipe, Int. J. Heat Mass Transfer, Vol. 51, pp. 661-671.

(a).

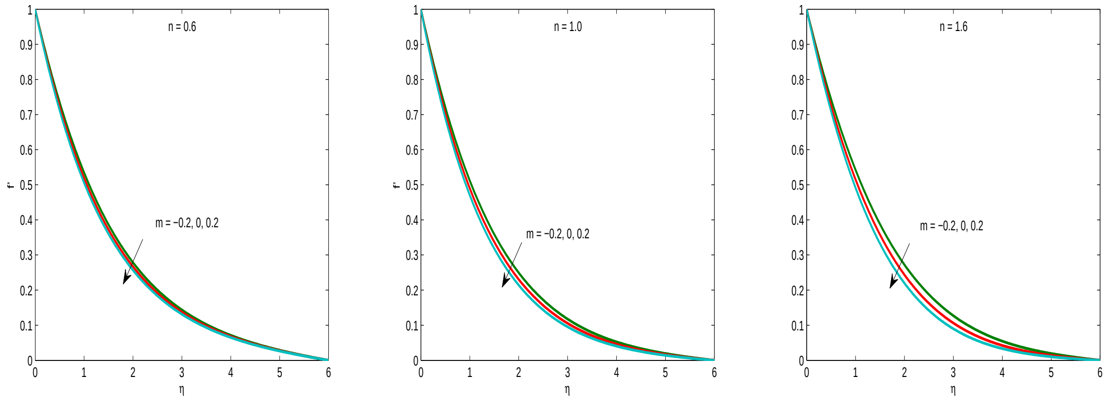

(b).

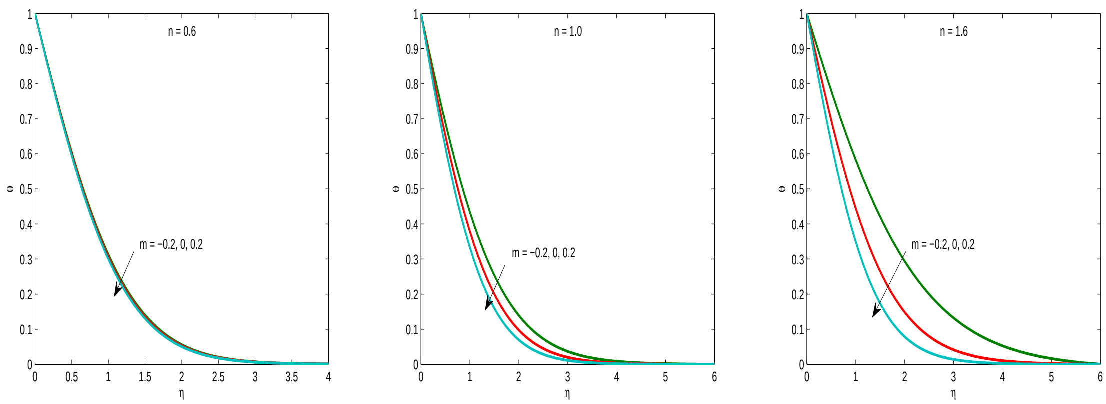

(c).

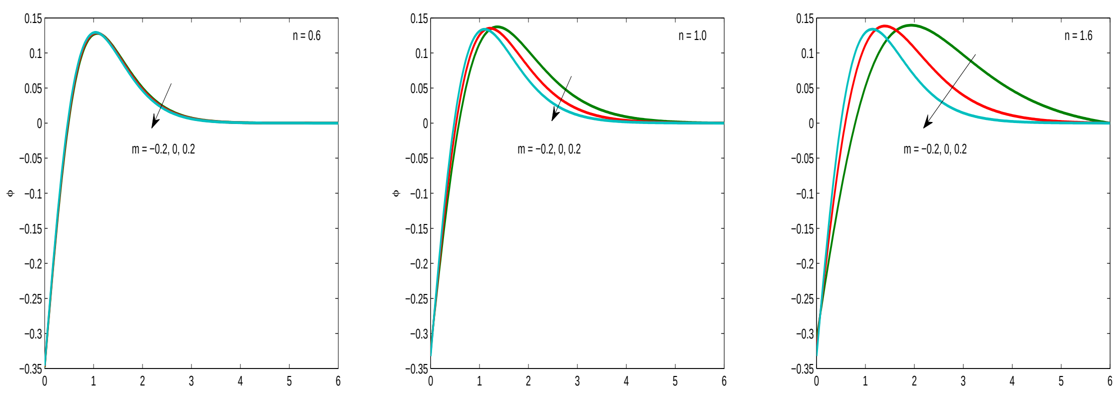

Figure 1. Effect of m on (a) velocity, (b) temperature, (c) concentration for pseudoplastic, Newtonian and dilatant fluids.

(a).

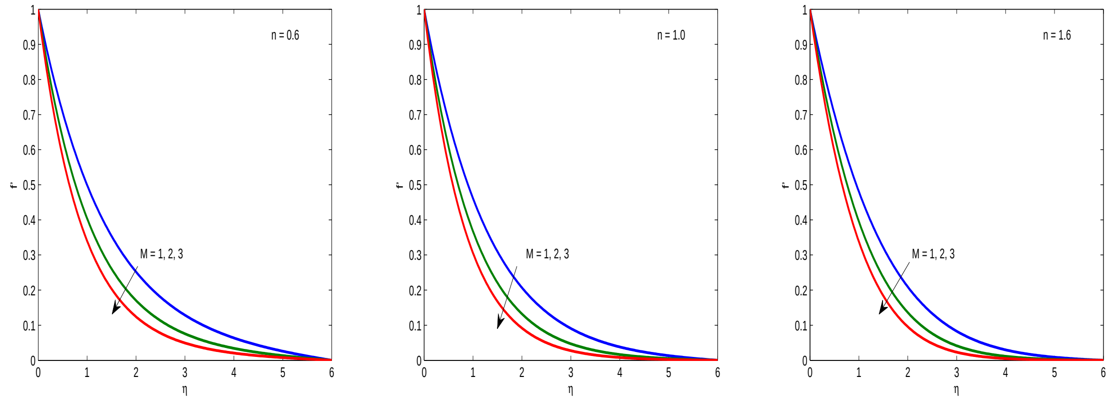

(b).

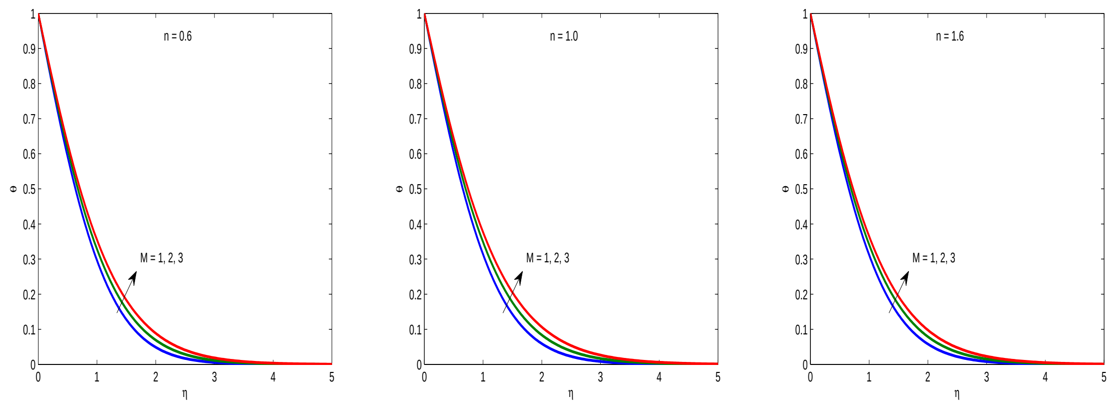

(c).

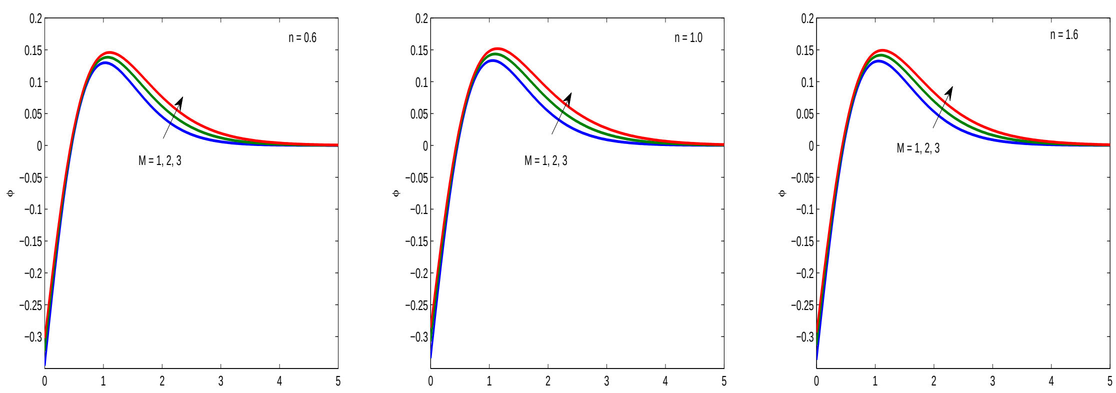

Figure 2. Effect of M on (a) velocity, (b) temperature, (b) nanoparticle volume fraction for pseudo-plastic, Newtonian and dilatant fluids.

(a).

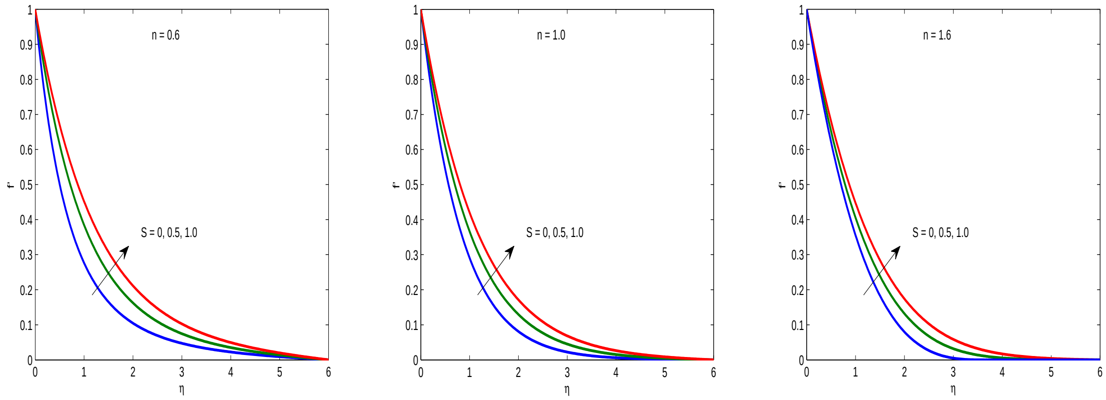

(b).

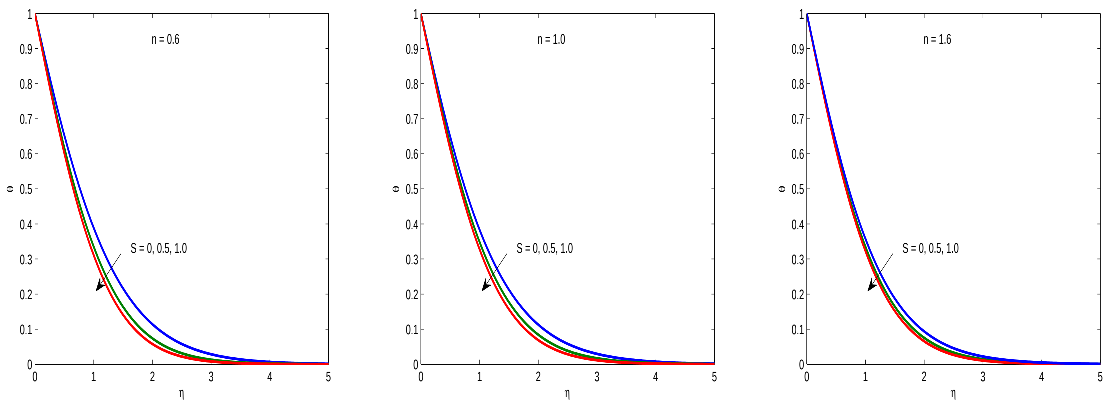

(c).

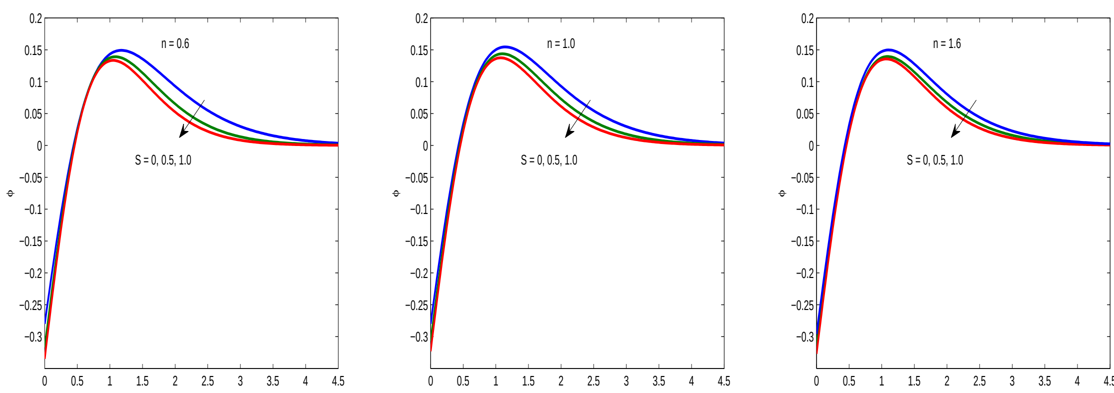

Figure 3. Effect of S on (a) velocity, (b) temperature, (c) concentration for pseudoplastic, Newtonian and dilatant fluids.

(a).

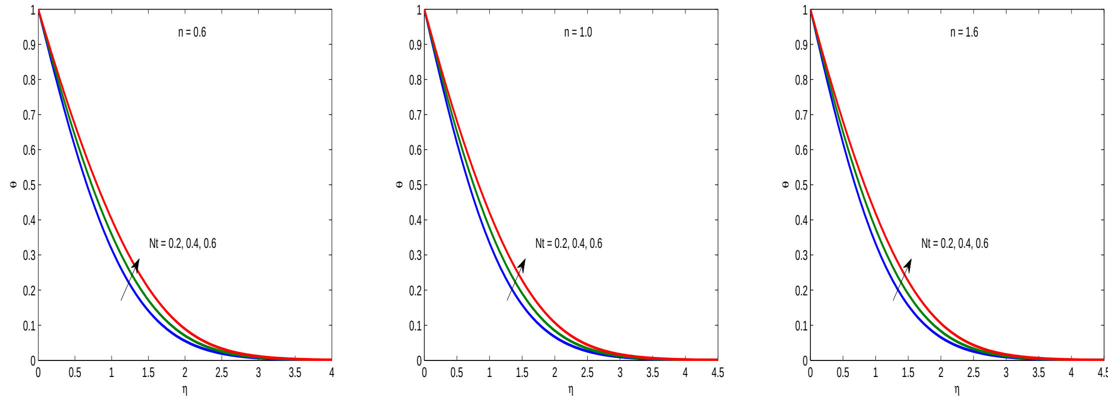

(b).

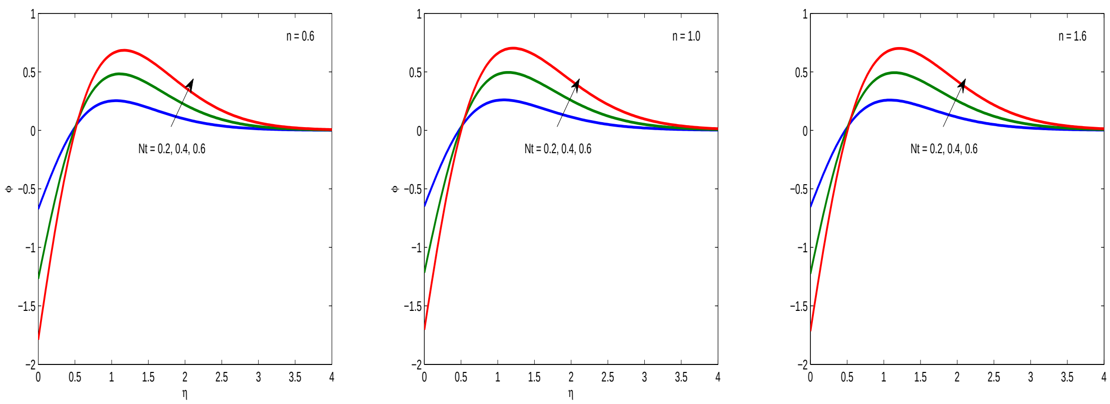

Figure 4. Effect of Nt on (a) temperature, (b) concentration for pseudo-plastic, Newtonian and dilatant fluids.

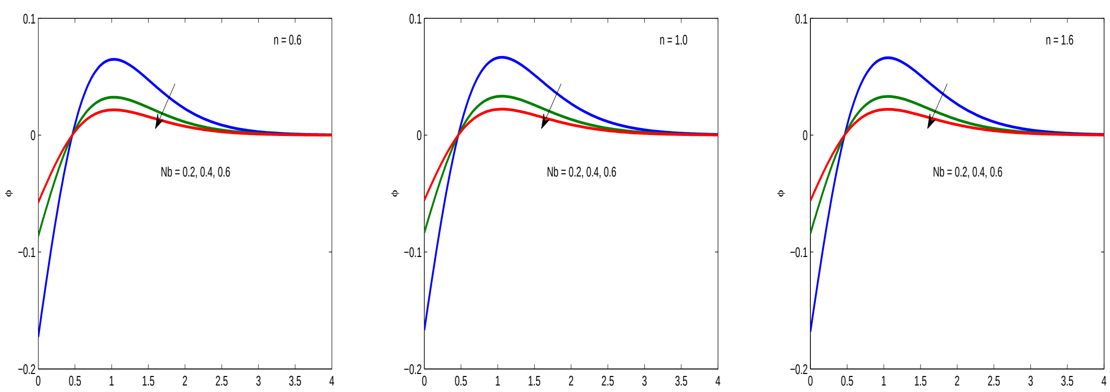

Figure 5. Effect of Nb on temperature profiles for pseudoplastic, Newtonian and dilatant fluids.

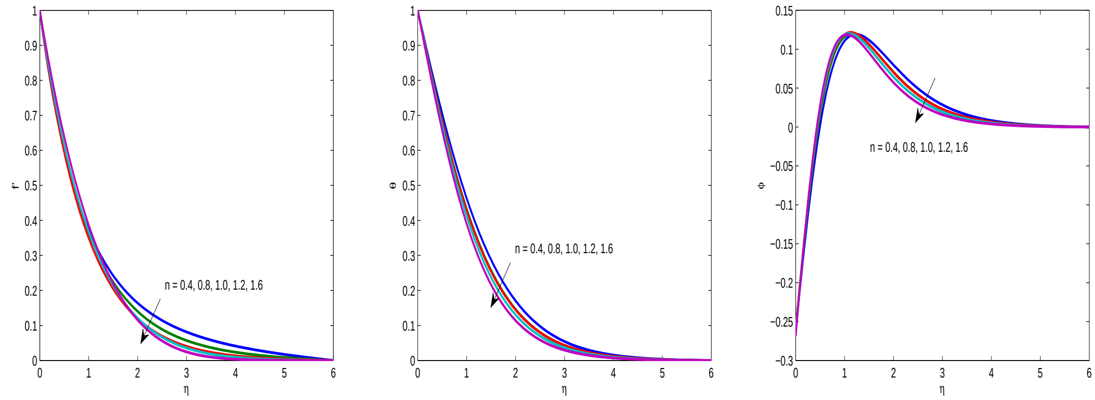

((a)) velocity **((b))** temperature **((c))** concentration

Figure 6. Effect of n on the velocity, temperature and concentration profiles.

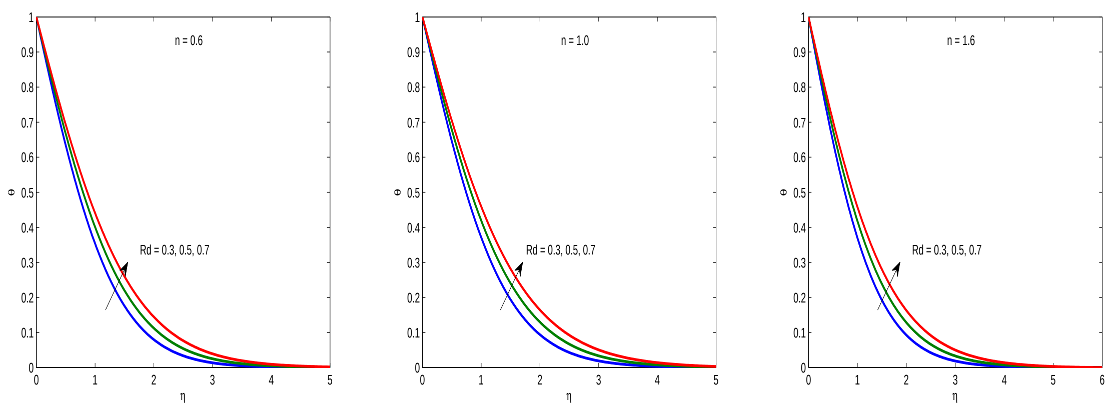

Figure 7. Effect of Rd on temperature profiles for pseudoplastic, Newtonian and dilatant fluids.

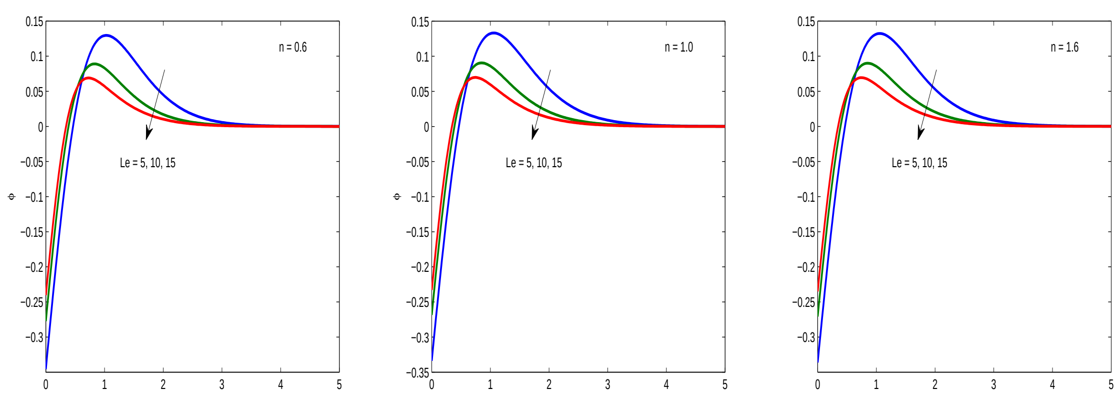

Figure 8. Effect of Le on concentration profiles for pseudoplastic, Newtonian and dilatant fluids.